Runaway Electrons in JET - Status of RE Data after the End of JET Operations in 2023

V.V. Plyusnin[1*§], C. Reux[*§], V.G. Kiptily[*§], A.E. Shevelev[*§], S. Gerasimov[*§], T. Craciunescu[*§], A. Huber[*§], O. Ficker[*§], S. Silburn[*§], J. Mlynar[*§], M. Lehnen[*§], S. Jachmich[*§], U. Sheikh[*§], E. Joffrin[*§], P. J. Lomas[*§], E. Nardon[*§], A. Boboc[*§], M. Baruzzo[*§], JET contributors* and the EUROFusion Tokamak Exploitation Team[§].

EUROFusion Consortium, JET, Culham Science Centre, Abingdon, OX14 3DB, UK

*(1) Instituto de Plasmas e Fusão Nuclear, Instituto Superior Tecnico, Universidade de Lisboa, Lisboa, Portugal; * See the author list of "Overview of T and D-T results in JET with ITER-like wall" by C.F. Maggi et al. to be published in Nuclear Fusion special issue: Overview and summary papers from the 29th Fusion Energy Conference (London, UK, 16-21 October 2023); §See the author list of E. Joffrin et al 2024, accepted for publication in Nuclear Fusion*

E-mail: vladislav.plyusnin@ipfn.ist.utl.pt

INTRODUCTION AND BACKGROUND

Disruptive terminations of plasma discharges pose severe threats to the device integrity in future operations of International Thermonuclear Experimental Reactor (**ITER**). Disruptions can cause dangerous excessive electromagnetic forces, heat loads and generation of the intense beams of relativistic runaway electrons (**RE**). Localized interaction of such beams with surrounding plasma facing components (**PFC**) inevitably will result in their inacceptable damage. To avoid/suppress RE generation and mitigate other disruption detrimental consequences the Disruption Mitigation System (**DMS**) is under design in ITER. It is based on impurities injection in the form of solid shattered pellets (**SPI**) and Massive Gas Injections (**MGI**). Development of DMS requires advanced understanding of the physics of RE and their interaction with plasma, solid pellets and neutral gases (fuel and injected impurities). For this purpose the parameters of disruption generated RE collected during disruptions till to the end of JET operations in 2023 were compiled into joint database. It includes parameters of more than 2300 RE generation events in major disruptions before and after divertor installation (**JET** with **O**riginal **P**lasma **S**hape, **JET OPS, JET** with $S_{pl} \leq 4.7$ m^2, see table 1), with metal and carbon limiters and with ITER-like Wall (**JET-ILW**), in spontaneous disruptions and those triggered by slow gas puff, MGI and SPI. This report presents current status of analysis of RE data in JET.

HISTORICAL SUMMARY ON RE GENERATION DURING JET OPERATIONS

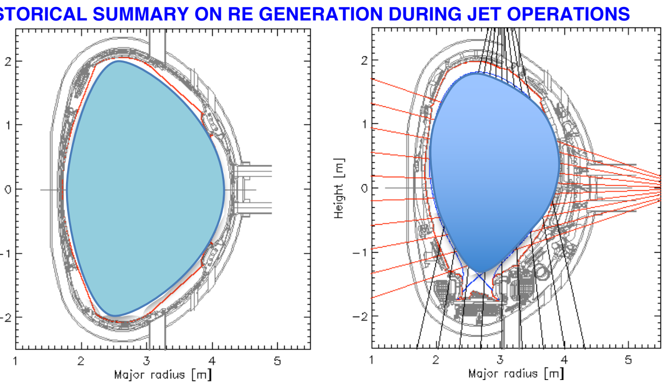

***Figure 1**. The JET plasma cross-sections with original shape before divertor installation (JET OPS, $S_{pl} \approx 6.6$ m^2, left chart) and with divertor coils installed inside of the vacuum vessel (JET divertor, $S_{pl} \leq 4.7$ m^2, right).*

Operational phase & configurations	Period	Final shot number	Number of detected RE events
Limiter only **(JET OPS, $S_{pl} \leq 6.6$ m^2)**	Operations till to August 87	#12106	≈ 320 events
Limiter + X-Point (SN, DN) **(JET OPS, $S_{pl} \leq 6.6$ m^2)**	August 87 - February 92	#28791	≈ 560 events
Divertor – MKI (**$S_{pl} \leq 4.7$ m^2**)	March 94 - June 95	#35778	≈ 130 events
- MKIIA, AP **JET-Divertor**	May 1996 – Feb 98 – Sept 98	#45155	≈ 220 events
- MKIIGB	July 1998 - March 2001	#54549	≈ 230 events
- MKIIGB SR	Jul 2001 - Mar 2004; Aug 2005 - Apr 2007	#63445	≈ 200 events
- MKII HD	Carbon wall ends 23-Oct-2009	#79853	≈ 340 events
- MKII ILW **JET-ILW**	ILW from July 2011, RE study ends 18 December 2023	#105841	≈ 330 events

Table 1. A survey of JET operational stages and number of registered RE generation events in disruptions during each phase.

- **≈330** disruptions with RE at disrupted currents up to 3MA during JET-ILW SPI-MGI experiments have been dedicated to studies of interaction of RE beams with MGI or SPI of D_2 and He, Ar, Ne, Xe, Kr or their mixture with D_2.
- All other unintentional disruptions in JET-ILW have been mitigated with MGI (10%Ar+90%D).

INSTRUMENTATION

RE interacting with plasma particles and PFC lose energy and produce the X-ray emission in a wide energy range: from soft X-rays (SXR) till to multi-MeV energies of hard X-rays (HXR) or γ-rays; HXR energy corresponds to the energy of electrons: $\mathbf{E_{HXR} \leq E_{RE\_MAX} - m_e c^2}$; Photo-neutrons (nY) are also produced when γ's interact with PFC and plasma particles and when the photon energy is higher than the neutron bound energy of target nuclei ε_n: $\mathbf{E_n = E_{HXR} - \varepsilon_n}$. Binding energies for different materials in JET are: **D_2 – 2.2 MeV; Be – 1.7 MeV; C – 18.7 MeV; Ar – 9.9 MeV; Ni – 12.0 MeV; Cu – 10.6 MeV; W – 7.4 MeV, Ne – 8 MeV**.

Figure 2 presents layout of diagnostics sets used for measurements of RE parameters in the JET experiments: 5 scintillation time-resolved HXR monitors, for neutron rates fission chamber monitors (^{235}U and ^{238}U) at 3 different locations (N1, N2 & N3 - Oct. 2,6,8) operating in a current mode with 0.0001 sec time resolution (Figure 2, left chart).

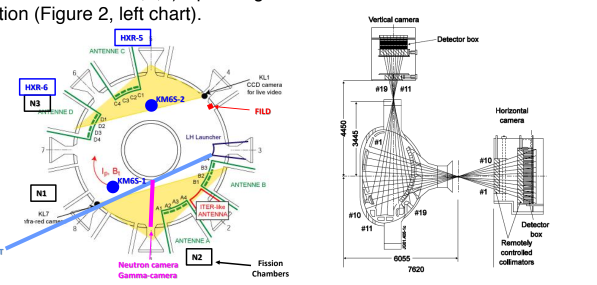

__Figure 2.__ Layout of JET diagnostics used in RE studies (left chart) and JET neutron/γ-profile monitor setup (right chart): 2 cameras, vertical and horizontal, with 9 and 10 detectors (corresponding Lines of Sight (LoS) are shown).

Horizontally and vertically viewing NaI(Tl), Bi_4GeO_{12} (aka BGO, Oct. 8) and $LaBr_3$ spectrometers; JET neutron/γ-rays profile monitor in Oct.1 (Figure 2, right chart). Each camera has 2 detectors: NE213 – for neutron and HXR measurements, and CsI detector for HXR registration. Fan-shaped array of remotely adjustable collimators with two apertures (Ø10 & 21 mm) provide the space resolution: ~8 (or ~15) cm (in the centre). CsI(Tl) scintillators (for HXR/gammas) equipped with fast digital data acquisition system: t ≈ 1 ms. HXR

2D imaging system enables the reconstruction of evolution in time and space of the RE beam; Several sets of SXR cameras have been used to produce SXR tomography of the RE beams images in-flight.

REFERENCE MODEL FOR ANALYSIS AND MAIN TRENDS IN RE GENERATION PARAMETERS DURING DISRUPTIONS IN JET OPERATIONS

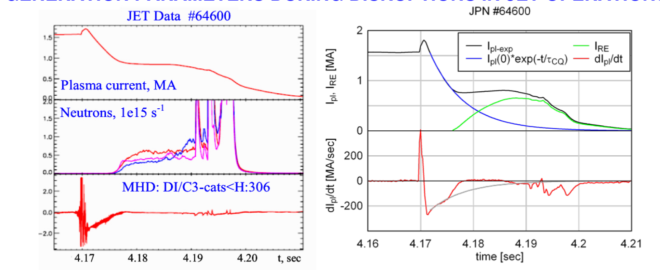

***Figure 3.** Spontaneous current rise disruption in JET with CFC PFC (left) and reference model for analysis of RE generation dynamics (right)*

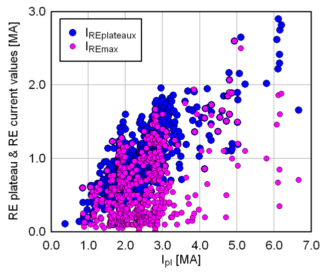

***Figure 5** Maximal values of RE plateaux and RE currents inferred from measured plateau during disruptions triggered by GIM puff and MGI+SPI in JET operations.*

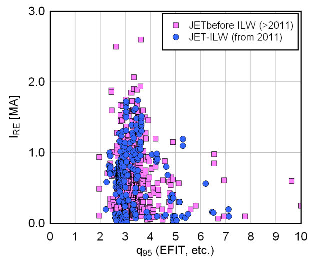

***Figure 6.** Maximal values of RE currents inferred from measured all types of disruptions in JET plotted vs. safety factor q_{95}.*

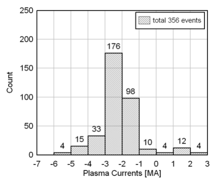

***Figure 7.** Statistics on RE generation events during disruptions in JET OPS detected as emission of HXR & neutron Yield*

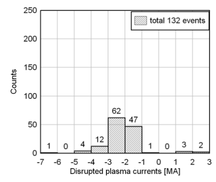

***Figure 8.** Statistics on RE generation events in JET OPS detected as deviation from exponential plasma current decay and with HXR & neutron Yield*

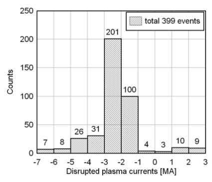

***Figure 9.** Statistics on RE generation events during disruptions in JET OPS detected as long time persisting RE current plateau (+HXR & nYield).*

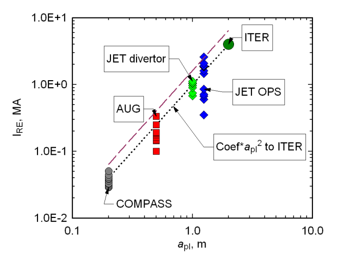

***Figure 10.** Trend in RE generation depending on plasma radius in different devices with extrapolation to ITER plasma radius (1≤Coef≤1.6).*

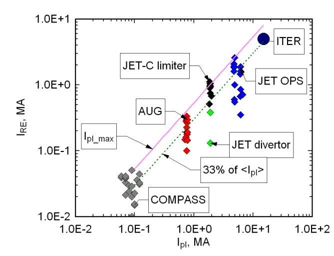

***Figure 11.** Conversion of the resistive plasma currents into RE beams inferred from the data obtained on JET and European tokamaks (1≤Coef≤1.6).*

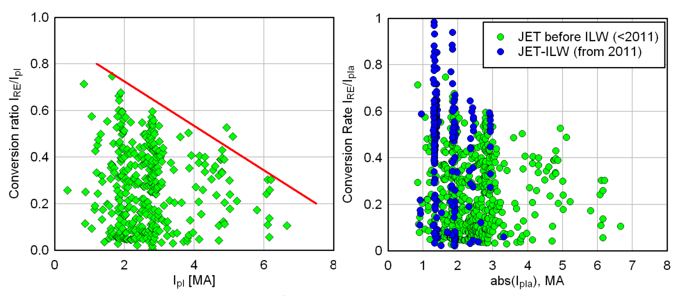

***Figure 12.** Trend in conversion of the resistive plasma current into RE one in JET OPS suggests significantly decaying dependence on plasma currents (left), as well as for all stages of JET operations (Divertor, CFC, ILW, MGI+SPI) (right).*

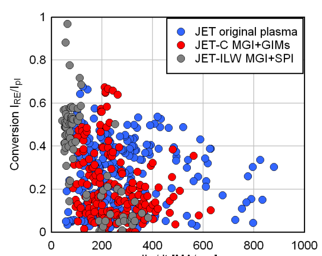

***Figure 13.** Decreasing trend in conversion ratio dependence on time derivative of disrupted plasma currents has been found for all JET operation stages.*

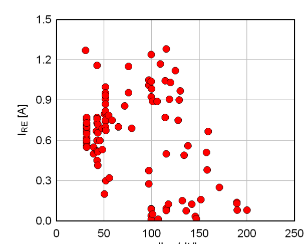

***Figure 14.** Optimization of MGI and SPI disruption scenarios resulted in high RE currents, especially for low disrupted currents in magnetic fields 3 T and higher values*

ROLE OF B_{TOR} AND ITS DIRECTION ON RE GENERATION.

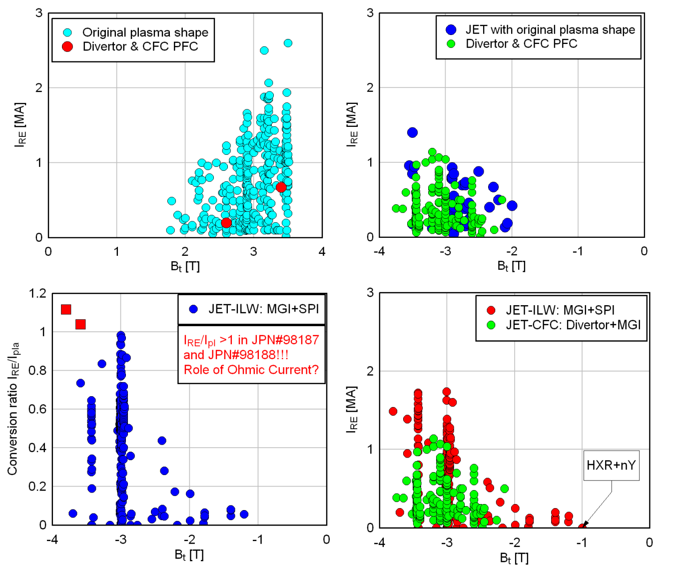

***Figure 15.** RE current values measured during spontaneous disruptions, those triggered by slow GIM puff and MGI+SPI and plotted as maximal I_{RE} and as conversion ratio I_{RE}/I_{pl} vs. B_t with different directions in JET disruptions. Optimization of MGI-SPI JET RE experiments obviously demonstrated absence of the "2T-threshold" on magnetic field for RE generation.*

EFFECT OF CURRENT QUENCH DYNAMICS AND PLASMA GEOMETRY DYNAMICS ON RE GENERATION: JET EXPERIMENTS AND SIMULATIONS

Disrupted plasmas move fast in space (vertical and horizontal) with changes in many parameters: radius, total inductance, magnetic flux, etc. These evolutions revealed definite effect on RE generation dynamics.

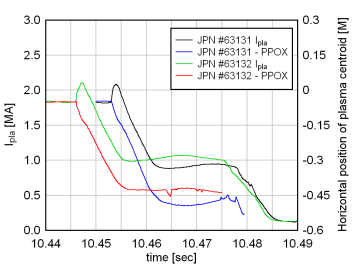

***Figure 16.** Evolutions of plasma centroids (PPOX) and currents in disrupted pulses with RE generation: JPN#63131 & JPN63132*

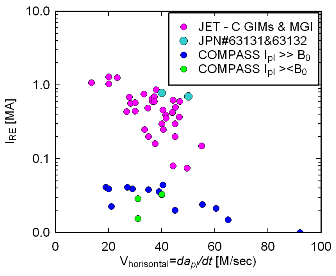

***Figure 17.** Effect of the plasma centroid dynamics in horizontal direction ($V_{horizontal}=da_{pl}/dt$) on RE generation efficiency in tokamaks*

Simulations on disruption evolutions were carried out using following model:

$$\frac{dn_{RE}}{dt} = \lambda_R + \left(\gamma_{AV} - \frac{1}{\tau_{RE}}\right) \cdot n_{RE} \qquad (1),$$

$$I_{pla}(t) + \frac{L_p(t)}{R_{pl}(t)}\frac{dI_p}{dt} + 0.5 \cdot I_p(t)\frac{dL_p}{dt} = 0 \qquad (2),$$

$$\rho\frac{dv}{dt} = \sum_i F_i \qquad (3);$$

Where $F_1 = 2\pi R(t) I_p(t) \cdot B_V$, $\quad B_V = \mu_0 \frac{I_p(0)}{4\pi R_0}\left(ln\frac{8R_0}{a_{pl}(0)} + \beta_p(0) + \frac{l_i(0)}{2} + 2\right)$,

$F_2 = \mu_0 \frac{I_p^2(t)}{2}\left(ln\frac{8R(t)}{a_p(t)} + \beta_p^*(t) + \frac{l_i^*(t)}{2} + 2\right)$ $\quad \beta_p^*(t) = \beta_p(t) + \beta_{RE}(t)$,

$L_p(t) = \mu_0 R_0(t)\left(ln\left(\frac{8R_0(t)}{a_p(t)}\right) + \beta_p^*(t) + \frac{l_i}{2} - 2\right)$, $\quad l_i = \ln(1.65 + 0.89c)$

$\gamma_{AV} = \frac{\frac{e}{mc}}{ln\Lambda\sqrt{\frac{3}{\pi}(Z_{eff}+5)}} \cdot \left(E_0(t) - E_{CR\_\infty} \cdot \frac{\gamma_0^2}{\gamma_0^2 - 1}\right)$ $\quad \beta_{RE}(t) = 8\pi^2 a_p^2 n_{RE} \frac{m_e c^2}{2\mu_0 I_p^2}\frac{(\gamma_0^2 - 1)}{\gamma_0^2}$

$\frac{dL_p}{dt} = \mu_0 \cdot \left[\frac{dR_0(t)}{dt} \cdot \left(\ln\left(\frac{8R_0(t)}{a_{pl}(t)}\right) - 2\right) + R_0(t)\left(\frac{\frac{dR_0(t)}{dt}}{R_0(t)} - \frac{\frac{da_{pl}(t)}{dt}}{a_{pl}(t)}\right)\right]$, $\quad \frac{\frac{dR_0(t)}{dt}}{R_0(t)} < 0$, $\frac{\frac{da_{pl}(t)}{dt}}{a_{pl}(t)} < 0$;

$2\pi R_0 E_{\parallel 0}(t) = -\left(L_{tot}(t)\frac{dI_p}{dt} + 0.5 I_p(t)\frac{dL_{tot}}{dt}\right)$; $\quad \gamma_0^2 = 1 + \left[\frac{e}{m_e c}\int E_0(t)dt\right]^2$

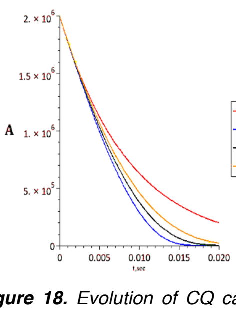

***Figure 18.** Evolution of CQ calculated with Eqs.(2-3) for different velocities of horizontal plasma toroid motion after disruption energy collapse during CQ*

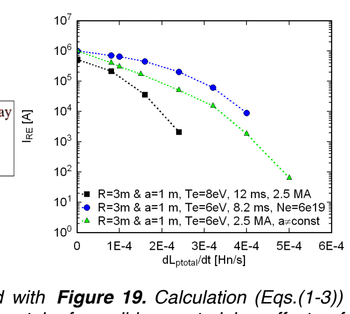

***Figure 19.** Calculation (Eqs.(1-3)) of possible constraining effects of plasma motion on RE generation via dL_p/dt: I_{RE} vs. dL_p/dt.*

SUMMARY

The database on RE in JET is under active study: latest JET experiments allow not only to design input parameters for numerical models, but also to avoid ambiguous interpretation of the early data. Collected data on RE generation events in JET disruptions represents an important part of JET experimental data. The first analysis of RE database has shown wide range of plasma parameters affecting the RE generation or increasing the efficiency of this process. In seems important to highlight the observed decreasing trend in conversion rate to RE current with increase of plasma currents and CQ rates. These trends require special attention in modelling.

ACKNOWLEDGEMENT

IST activities also received financial support from "Fundação para a Ciência e Tecnologia" through project UID/FIS/50010/2019. The views and opinions expressed herein do not necessarily reflect those of "Fundação para a Ciência e Tecnologia"

This work has been carried out within the framework of the EUROfusion Consortium and has received funding from the Euratom research and training programme 2014-2018 and 2019-2020 under grant agreement 633053. The views and opinions expressed herein do not necessarily reflect those of the European Commission.

ipfn INSTITUTO DE PLASMAS E FUSÃO NUCLEAR